

Molecular Dynamics Studies on HIV-1 Protease: Drug Resistance and Folding Pathways.

Fabio Cecconi¹, Cristian Micheletti¹, Paolo Carloni^{1,2} and Amos Maritan¹

(1) *International School for Advanced Studies (SISSA/ISAS), Via Beirut 2-4, I-34014 Trieste, INFN and “The Abdus Salam” International Centre for Theoretical Physics.*

(2) *International Centre for Genetic Engineering and Biotechnology (ICGEB) - AREA Science Park, Padriciano 99, I-34012 Trieste*

(November 17, 2018)

Drug resistance to HIV-1 Protease involves accumulation of multiple mutations in the protein. Here we investigate the role of these mutations by using molecular dynamics simulations which exploit the influence of the native-state topology in the folding process. Our calculations show that sites contributing to phenotypic resistance of FDA-approved drugs are among the most sensitive positions for the stability of partially folded states and should play a relevant role in the folding process. Furthermore, associations between amino acid sites mutating under drug treatment are shown to be statistically correlated. The striking correlation between clinical data and our calculations suggest a novel approach to the design of drugs tailored to bind regions crucial not only for protein function but also for folding.

I. INTRODUCTION

The human immunodeficiency virus encodes a protease (HIV-1 PR) cleaving the gag and the gag-pol viral polyproteins into enzymes and structural proteins [1]. The discovery that inhibition of this protease (a homodimer of 198 amino acids) causes the formation of non-infectious virus particle has prompted an enormous effort to design efficient inhibitors against AIDS attack [2]. Currently, five antiviral agents are approved by FDA: Saquinavir (SQV), Zidovudine (ZDV), Zalcitabine (ZCZ), Didanosine (DDI) and several others are under clinical trials [1–4]. Therapeutic benefit is unfortunately short-lived as the virus strains - evolving under drugs’ selective pressure - encode HIV-1 PR multiple mutants with low drugs affinity [1,4–8]: mutants resistant to protease inhibitors can emerge in vivo already after less than one year [5]. The problem of drug-resistance persists also when a combination of PR and reverse transcriptase (RT) inhibitor are used.

The occurrence of mutations withstanding antiviral drugs is not a mere consequence of drug action, rather it results from viral replication itself [5]. Indeed, mutations are found rather irrespective of drug structural diversity involving virtually every protein domain: this is the case for HIV-1 PR mutants which are resistant against FDA approved drugs [4]. Among such mutations, a few involve the active site (residue 25 - aspartic acid [6]) while the others belong to protein regions away from it.

By means of molecular dynamics (MD) simulations within the framework introduced in Ref. [9] (see next section), we show here that the positions where these mutations occur play a key role in the proximity of temperatures where the specific heat peaks occur. Moreover, we shall argue that residues involved in a frequently observed covariant mutation [5], are statistically correlated. Indeed, while the study of the native state structure can lead to a rational design of drugs binding the active site (or otherwise disrupt the biological function of the agent by acting on its native structure) the analysis of the folding pathways can provide fundamental information [10]. In particular, it can reveal, as in the case of HIV-1 PR, the presence of kinetic bottlenecks associated to severe entropy reduction that inhibits the progress toward the native state. These bottlenecks represent the most delicate part of the folding process. They are followed by the sudden formation of specific native-like protein sub-regions and afterwards the folding process proceeds rapidly until another bottleneck is reached. The identification of sites involved in the bottlenecks and their correlation with the active site is crucial pharmaceutically because they are the ideal targets of effective drugs. From this point of view, due to the large amount of data available on drug resistance, HIV-1 PR is an excellent candidate to validate our automatic strategy to identify key folding sites. In the following, we shall present evidence showing that the crucial sites can be identified with good statistical confidence. The framework introduced here is general and, applied to other viral proteins, ought to be useful for suggesting which sites should be preferentially targeted by effective drugs.

II. THEORY

The strategy adopted here to identify the crucial sites for the folding and assembling of HIV-1 PR is based on a recent theoretical framework [9,11] that allows to capture the main features of the folding process by a simplified description of both the protein structure and the folding dynamics. At the basis of the method is the observation that the topology of the native state plays a crucial role in steering the folding process [9,12–17]. This statement is supported by an increasing amount of experimental evidence. Perhaps, the most notable examples are: (a) the close similarity of the transition-state conformations of proteins having structurally-related native states (despite the very poor sequence similarity) [18,19] and (b) the strong influence that certain simple topological properties, such as the contact order, have on protein folding rates [20]. Such observations, and others summarised in the recent review of D. Baker [21], complement the findings of Anfinsen, who established that a protein’s amino acid sequence uniquely encodes its native state [22]. Indeed, since the topology of the native state influences the folding process, the amino acid sequence must also encode its possible folding pathways.

We focus our attention on the topological rate-limiting steps along the pathways from unfolded states to the native one. Such bottleneck stages, are usually found in correspondence of non-local amino acid interactions that require the overcoming of a large entropy barrier (due to the flexibility of the peptide chain intervening between them); the formation of such crucial contacts acts as a nucleus for the establishment of further native interactions and leads to a rapid progress along the folding reaction coordinate until another barrier is met.

It is striking that the sites involved in the topological bottlenecks are those where the largest changes in the folding kinetics are observed in site-directed mutagenesis experiments [10], as first established for CI2 and Barnase [9]. This shows that nature has carefully optimised the protein sequence so to exploit the conformational entropy reduction accompanying the folding process [23] through the careful choice of the amino acids forming the crucial contacts.

With the purpose of identifying the key sites we investigate the topological obstacles encountered during the formation of the native HIV-1 PR structure. Such sites are, intuitively, the ideal candidate targets of effective drugs, as they take part to the most delicate steps of the folding process. This fact was first recognised by Anfinsen in connection with the staphylococcal nuclease [22]. The most effective strategy to prevent the protein formation is acting on residues involved in the key contacts and undermining the formation/overcoming of bottleneck stages. One of the distinctive features of the HIV virus is the extremely high rate of mutations. The capability of encoding several mutants provides a possibility for HIV-1 PR to elude the disruptive action of the drug by intervening on the key sites. This seems an unavoidable countermeasure since the viable mutants (i.e. those with native-like enzymatic activity) retain the original native structure and hence, arguably, encounter the same bottlenecks as the wild-type. Within this framework, the lapse of time during which the drug therapy is temporarily effective, corresponds to the time taken by the virus to encode, through random mutations, a mutant form of HIV-1 PR where the crucial sites have been fine-tuned to overcome not only the kinetic bottlenecks (as for the wild type) but also the additional drug attack. The key sites identified through the method explained in the next sections, have been compared with the known key mutating positions of HIV-1 PR, finding a highly significant correlation between the two of them. In addition, previously unexplained co-variant mutations seen in HIV-1 PR are explained as arising due to the correlation between distinct topological bottlenecks.

III. METHODS

The model that we adopted encompasses an energy-scoring function of the Go-type [24]. This is one of the simplest energy functionals and provides a natural topological bias to the native state by rewarding the formation of native pairwise interactions. In the version used here, which is a generalization of ref. [9] apt for molecular dynamics studies, the cooperativity of the folding process is enhanced by the introduction of repulsive non-native interactions. In our Hamiltonian, each pair of non-consecutive amino acids interacts with the following strength:

$$5V_0\varepsilon_{ij}^N \left[\left(\frac{r_{ij}^N}{r_{ij}} \right)^{12} - \frac{6}{5} \left(\frac{r_{ij}^N}{r_{ij}} \right)^{10} \right] + V_1(1 - \varepsilon_{ij}^N) \left(\frac{r_0}{r_{ij}} \right)^{12}, \quad (1)$$

where $r_0 = 6.8\text{\AA}$, $r_{i,j}^N$ denotes the distance of C_α atoms of amino acids i and j in the native structure and ε_{ij}^N is the native contact map, whose entries are 1 (0) if i and j are (not) in contact in the native conformation (i.e. below or above 6.5\AA). V_0 and V_1 are constants controlling the strength of interactions ($V_0 = 20$, $V_1 = V_0/400$ in

our simulations). In addition, the peptide bond between two consecutive amino acids, i , $i + 1$ at distance $r_{i,i+1}$ is described by the unharmonic potential:

$$\frac{a}{2}(r_{i,i+1} - r_d)^2 + \frac{b}{4}(r_{i,i+1} - r_d)^4 \quad (2)$$

with parameters $a = V_0$, $b = 10V_0$, and $r_d = 3.8 \text{ \AA}$ is the rest distance between consecutive C_α atoms.

It is important to notice that in Eq. (1) the formation of any native contact is rewarded in the same way, since V_0 does not depend on i and j . This choice is done deliberately, so that the only information entering Eq. (1) is the native contact map and not the types of interacting amino acids (i.e. no sequence information). While by construction, the minimum of the energy scoring function is achieved in correspondence of the native state, there is no *a priori* guarantee that the folding process, under the influence the pair interaction (1), occurs, on average, through the same stages encountered in nature, or even in a more sophisticated atomic MD simulation with *ab initio* force fields. Certainly, there are situations where the influence of the native-state topology on the folding process may be overridden by strong chemical propensities to form definite pairs of amino acids (such as disulfide bridges). In addition, given the explicit bias towards the native state, one should not expect that it would be possible to observe intermediate states with low concentration of native contacts. Aside from similar circumstances, it is appropriate to ask whether one can reproduce the key steps of the folding process by exploiting only the structural information of the native state. The basis and justification for the present study is the growing evidence that the above question has a positive answer. In fact, starting from the work of ref. [9] and later of refs. [12–17], it has become clear that the characterization of the transition states can be confidently done within a Go-model scheme for a variety of proteins.

In the present study, the starting structural model (target) is the free enzyme [5] which is a homodimer with each subunit composed by 99 residues, see Fig 1. Following [25], the crystallographic C2 symmetry was enforced during MD simulations to reduce the computational effort. The progress towards the fully folded (native) state was estimated in terms of the fraction of native contacts formed at any given time in the partially folded structure, Γ [26]. This quantity, also termed overlap, is defined as

$$Q = \frac{\sum_{i,j} \varepsilon_{ij}^N \cdot \varepsilon_{ij}^\Gamma}{\sum_{i,j} \varepsilon_{ij}^N}, \quad (3)$$

where ε^Γ is the contact matrix of Γ .

Constant temperature MD simulations were carried out for several decreasing temperatures from the unfolded to folded state of the protein. The equations of motion for the C_α atoms were integrated by a velocity-Verlet algorithm with time step $\Delta t = 0.01$ combined with the standard Gaussian isokinetic scheme [27]. We performed unfolding simulations within the same framework by starting from the native structure and taking it through a sequence of increasing temperatures (heat denaturation). The temperature was measured in reduced units V_0/k_B (being k_B the Boltzmann constant, and V_0 the energy of the native contacts in Eq. (1)). At each temperature, we let the system equilibrate from the last structure reached at the previous run at a nearby temperature. Each equilibration involved $5 \cdot 10^5$ MD steps, a time much longer than the largest correlation times observed for the system. After equilibration, we sampled 4000 structures again at time intervals twice the estimated correlation time. At each temperature, we collected the energy histogram of such uncorrelated structures. Using the multiple histogram techniques [28], the energy measurements for all temperatures have been reweighted to provide optimal estimates of thermodynamic quantities such as the average energy and the specific heat (by differentiation of the former) for a continuous range of temperatures. The statistical significance of the data collected in our runs was checked by verifying that the reweighted thermodynamic quantities did not change by more than a few percent upon addition of energy histograms obtained from folding/unfolding simulations with different temperature schedules or initial conditions.

Within the approximation where the reaction coordinate is the internal energy, from the high temperature side, the slowest dynamics occurs at temperatures near the specific heat peak, with a relaxation time at least of order $D \cdot TC_V$, where D is a suitable coefficient dimension of seconds/Joules. Thus the contacts contributing more to the specific heat peak are identified as the key ones belonging to the folding bottleneck and sites sharing them as the most probable to be sensitive to mutations. Furthermore, by following several individual folding trajectories (by suddenly quenching unfolded conformations below the folding temperature, T_{fold}) we ascertained that all such dynamical pathways encountered the kinetic bottlenecks described in the next section.

A reliable and convenient way to identify and characterize the kinetic bottlenecks is through the location of peaks and shoulders in the specific heat (which denote the overcoming of free energy barriers). Moreover, since the specific heat results from the contribution of each pair of native contacts, it is also useful to monitor the formation of each native interaction throughout the folding process. Indeed, the probability of formation of a native contact is a

decreasing function of T and has a sigmoidal shape fitted by suitably shifted hyperbolic tangent (see Fig. 2). The smooth interpolation allows to identify a crossover temperature, T_0 , where the slope reaches its maximum, C_0 (that is the inflection point of the curves in Fig. 2). T_0 defines a local “transition” temperature at which each contact is locked, whereas C_0 , which represents the “rapidity” of its formation, can also be regarded as a measure of the local contribution to the specific heat.

IV. RESULTS

At very low temperatures, the observed structures have nearly 100 % native-state similarity, measured as the fraction Q of established native contacts (Eq. 3). Further increase in temperature causes structural rearrangements into a configuration that cannot be assembled into a dimer anymore (Fig. 3): the number of subunit-subunit contacts vanished and the two subunits behaved independently. The dissociation mechanism is well described by Fig. 4 where we report, for several temperatures, the fractional occupation of native contacts for the individual subunits and at the monomer-monomer interface. The dissociation is also signalled by an abrupt increase of the specific heat of the dimer, see inset of Fig. 5, (this defines the dissociation temperature T_{diss}). A typical structure at this temperature is shown in Fig. 3a. At even higher temperatures ($T = 1.4T_{diss}$), a large increase of specific heat is observed, indicating the presence of a strong transition of the single subunits [29], see Fig. 5. This temperature is identified with the folding temperature, T_{fold} . Consistently with other studies on different proteins, the native overlap at T_{fold} was about 50 %. A typical structure at this temperature is shown in Fig. 3b.

A further set of bottlenecks is encountered at $T \approx 1.4T_{fold}$, where the formation of the three β -strands of HIV-1 PR is involved. Upon increasing the temperature one encounters β -sheet β_2 , then β_1 , then β_3 . It is found that the kinetic bottleneck for the a general β -sheet formation is not the establishment of the contact(s) closest to the β turn (that involves amino acids near in sequence) but it is located further away. A quantitative analysis of the amino acids most involved in the folding bottleneck is again obtained by monitoring during the folding/unfolding process each pair of amino acids which are in contact in the native state. Examples of the probability with which individual contacts are formed is shown in Fig. 2.

At each temperature where the dynamical evolution of the HIV-1 PR is followed, the formation probability of each native contact (fractional occupation) is calculated. Such quantities are 1 at very low temperatures (all native contacts always present) and decrease to zero at temperatures larger than the folding temperature. It may be anticipated that the rate of decrease as a function of temperature will not be the same for all contacting pairs. In particular, trivial local contacts between residues with a small sequence separation will have a large probability of being formed even at high temperatures. Our interest focuses on those contacts which show a dramatic increase of the fractional occupation near the folding transition. Those will be the key contacts responsible for the appearance of the specific heat peak. Examples of the fractional occupation for three native contacts is shown in Fig. 3. Given the monotonic behaviour of the fractional occupation, one may synthetically characterize the formation of each contacting pair by the temperature at which the point of inflection of the curve is seen and also by the slope at that very same point. Both data can be conveniently summarised in two scatter plots where the slope, C_0 , and the temperature of formation, T_0 , are reported for each residue taking part in native contacts. Such graphs are reported in the scatter plot of Fig. 6. Notice that, for each site, there are as many entries as the number of contacts involving it (a number that typically differs from site to site). Figure 6 clearly shows that there are clusters of contacts that are turned on at similar temperatures.

The bottlenecks for the folding process are identified by isolating the contacts having both a formation temperature, T_0 matching the location of the peaks and shoulders of the specific heat, and a high rapidity of formation, C_0 . Figure 6a reveals the presence of four distinct clusters of contacts. The first three, labelled β_1 , β_2 , β_3 , are associated with the formation of the three antiparallel β -sheets in HIV-1 PR. Their temperature of formation is about $1.4 \cdot T_{fold}$, and corresponds to the shoulder visible in the larger plot of the specific heat of Fig. 5. The sites sharing the most important contacts involved in such three bottlenecks are listed in Table I and highlighted in Fig. 3c, where a typical structure at $T = 1.4 \cdot T_{fold}$ is shown. It is interesting to see that T_0 is maximum for sites close to the β -turn, in accord with the intuitive expectation that the β formation is initiated at the turn. In Fig. 7 a,b and c, we have reported the values of C_0 only for the pairs of contacting sites in the β sheet. It is seen that the sites closest to the turn have a small formation rapidity. This can be understood since, being very close along the sequence, they can be easily formed/broken. The highest rapidity, C_0 , i.e. the highest difficulty of formation, is encountered typically 3-4 sites away from the turn. The corresponding contacts are then identified as the bottleneck for this particular folding stage. For the β -sheets, the bottlenecks involve amino acids that are typically 3-4 residues away from the turns.

Going back to Fig. 5, one observes that there is a fourth group of contacts around residues 30 and 86, labelled TB after “transition bottleneck”, that are formed cooperatively at the folding transition. The sites involved in the TB

contacts are listed in Table I. Among those contacts we have recorded the largest values of C_0 , as shown more clearly in Fig. 6d. Again, we considered the sites with the highest values of C_0 as responsible for the main bottleneck of the folding process. The highest “rapidity” is measured in correspondence of contacts 29-86 and 30-84 (see also Fig. 7) which are, consequently, identified as the most crucial for the folding/unfolding process.

V. DISCUSSION

The sites involved in the main folding bottleneck (TB) are located at the active site of HIV-1 PR, which is targeted by anti AIDS drugs [6]. Hence, within the limitations of our simplified approach, we predict that changes in the detailed chemistry at the active site affect also a key step of the folding process. To counteract the drug action, the virus has to perform some very delicate mutations in correspondence of the key sites; within a random mutation scheme this requires many trials (occurring over several months). The time required for the biosynthesis of a mutant with native-like activity is even longer if the drug attack correlates with several bottlenecks simultaneously.

This is certainly the case for several anti-AIDS drugs. Indeed Table I summarises the mutations emerged for the FDA approved drugs [4]. Remarkably, among the first 23 most crucial sites predicted by our method and listed in Table I, there are 7 sites in common with the 16 distinct mutating sites of Table I. The probability that two sets of 16 and 23 sites randomly taken from a total population of 99 (the length of the HIV-1 PR monomer) share at least 7 sites is only 3 %. Also note that, all the mutation sites of Table I except 82,35,36 and 90 fall within a mismatch of at most one position from the sites of Table II. These results highlight the highly statistical correlation between our prediction and the evidence accumulated from clinical trials.

All mutations causing resistance involve crucial residues for the main folding bottleneck, (particularly residue 84) in combination with key sites for one or more of the β sheets. Mutation in this sites are expected to modify the energetics and structure of partially folded states. In contrast the folded state appears to be weakly affected by specific mutations, such as M46I, L63P, V82T, I84V, which lead to a C_α RMS distance of 0.5 Å from the wild-type [35,36]. In the light of these results, it is possible to interpret the experimental evidence for the existence of correlations between mutations at residue 82 and residues 10, 54, 71 as correlations between the main kinetic barrier, TB and the others β_1 , β_2 , β_3 . The large separation of these associated sites, both along the sequence and in space, suggests that their correlations arise by virtue of the folding process itself. This kinetic effects is particularly clear in one of these cases, namely the co-mutation of sites in the TB and at residue 10, which occurs under IND therapy. The mediator of the correlation is residue 23 which takes part to two bottlenecks: TB and β_1 through direct contact with residues 84 and 10, respectively. Co-varying mutations between the two sites are observed because changes in TB will affect the environment of the other key site 10, which has to mutate accordingly.

VI. CONCLUSIONS

The strategy presented here allows both to identify the bottleneck of the folding process and to explain their highly significant match with known mutating residues. This approach should be readily applicable to identify the kinetic bottlenecks of other viral enzymes of pharmaceutical interest, thus aiding the development of novel inhibitor targetting the kinetic bottlenecks. This is expected to enhance dramatically the difficulty for the virus to express mutated proteins which still fold efficiently into the same native state with unaltered functionality.

Acknowledgements This work was supported by INFM and MURST.

-
- [1] Gulnik S., Erickson J.W., Xie D. *Vitam Horm.*, **58**, 213-56 (2000).
 - [2] Wlodawer A., Erickson J.W. *Annu Rev Biochem*, **62**, 543-585, (1993) and references therein.
 - [3] P. Reddy and J. Ross, *Formulary*, **34**, 567-675 (1999).
 - [4] Ala P.J, et al. *Biochemistry* **37**, 15042-15049, (1998).
 - [5] Condra JH et al. *Nature*, **374**, 569-571. (1995)
 - [6] Brown A.J., Korber B.T., Condra J.H., *AIDS Res. Hum. Retroviruses* ,**15**, 247-53 (1999).
 - [7] Durant J., et al. *Lancet* , **353**, 2195-9. (1999)
 - [8] Boucher C., *AIDS* **10**, S15-9 (1996)

- [9] Micheletti, C., Banavar, J.R., Maritan, A. & Seno., F. *Phys. Rev. Lett.* **82**, 3372-3375, (1999).
- [10] Fersht A.R., *Proc. Natl. Acad. Sci. USA*, **92**, 10869-10873 (1995).
- [11] Maritan, A., Micheletti, C. & Banavar, J.R. *Phys. Rev. Lett.*, **84**, 3009-3012, (2000).
- [12] O. V. Galzitskaya and A. V. Finkelstein, *Proc. Natl. Acad. Sci. USA*, **96**, 11299-11304 (1999).
- [13] V. Muñoz, E. R. Henry, J. Hofrichter and W. A. Eaton, *Proc. Natl. Acad. Sci. USA*, **95**, 5872 (1998).
- [14] Alm E. and Baker D. *Proc. Natl. Acad. Sci. USA* **96**, 11305-11310 (1999).
- [15] Chiti, F., et al. *Nature Struct. Biol.*, **6**, 1005-1009 (1999).
- [16] J. C. Martinez, M. T. Pisabarro and L. Serrano. *Nature Struct. Biol.*, **5**, 721-729 (1999).
- [17] C. Clementi, H. Nymeyer and J. N. Onuchic, *J. Mol. Biol.*, **298**, 937-953 (2000).
- [18] J. C. Martinez and L. Serrano, *Nature, Struct Biol*, **6**, 1010-1016 (1999)
- [19] D. S. Riddle et al. , *Nature Struct. Biol.* , **6**, 1016-1024 (1998).
- [20] K. W. Plaxco, K. T. Simons, and D: Baker, *J. Mol. Biol.*, **277**, 985-994 (1998)
- [21] D. Baker, *Nature*, **405**, 39-42 (2000)
- [22] Anfinsen, C. *Science* **181**, 223-230 (1973).
- [23] P. G. Wolynes J. N. Onuchic and D. Thirumalai, *Science* **267**, 1619-1620 (1995);
- [24] Go, N. & Scheraga, H.A. *Macromolecules* **9**, 535-542, (1976).
- [25] Clementi C., Carloni P. and Maritan A., *Proc. Natl. Acad. Sci. USA*, **96** 9616-9621 (1999).
- [26] H. S. Chan and K. A. Dill, *Proteins: Str. Funct. and Gen.*, **30**, 2-33 (1998).
- [27] Evans D. J., Hoover W.G., Failor B.H., Moran B., Ladd A.J.C., *Phys. Rev. A* **28** 1016-1021 (1983).
- [28] A. M. Ferrenberg and R. H. Swendsen, *Phys. Rev. Lett.* **63**, 1195 (1989).
- [29] M. H. Hao and H. A. Scheraga, *Physica A*, **244**, 124-145 (1997).
- [30] Molla A. et al. *Nat. Med.*, **2**, 760-6 (1996).
- [31] Markowitz M. et al. *J. Virol.* , **69**, 701-6 (1995).
- [32] Patick A. K., et. al. *Antimicrob. Agents Chemother.* , **40**,292-7 (1996) .
- [33] Tisdale M. at al. *Antimicrob. Agents Chemother.* ,**39**, 1704-10 (1995).
- [34] Jacobsen H. et al. *J. Infect. Dis.* , **173**, 1379-87 (1996).
- [35] Chen Z., Li Y., Schock H.B., Hall D., Chen E., Kuo L.C., *J Biol Chem*, **270**, 21433-21436 (1995).
- [36] Nair A.C., Miertus S., Tossi A., Romeo D., *Biochem. Biophys. Res. Commun.*, **242**, 545-551 (1998).

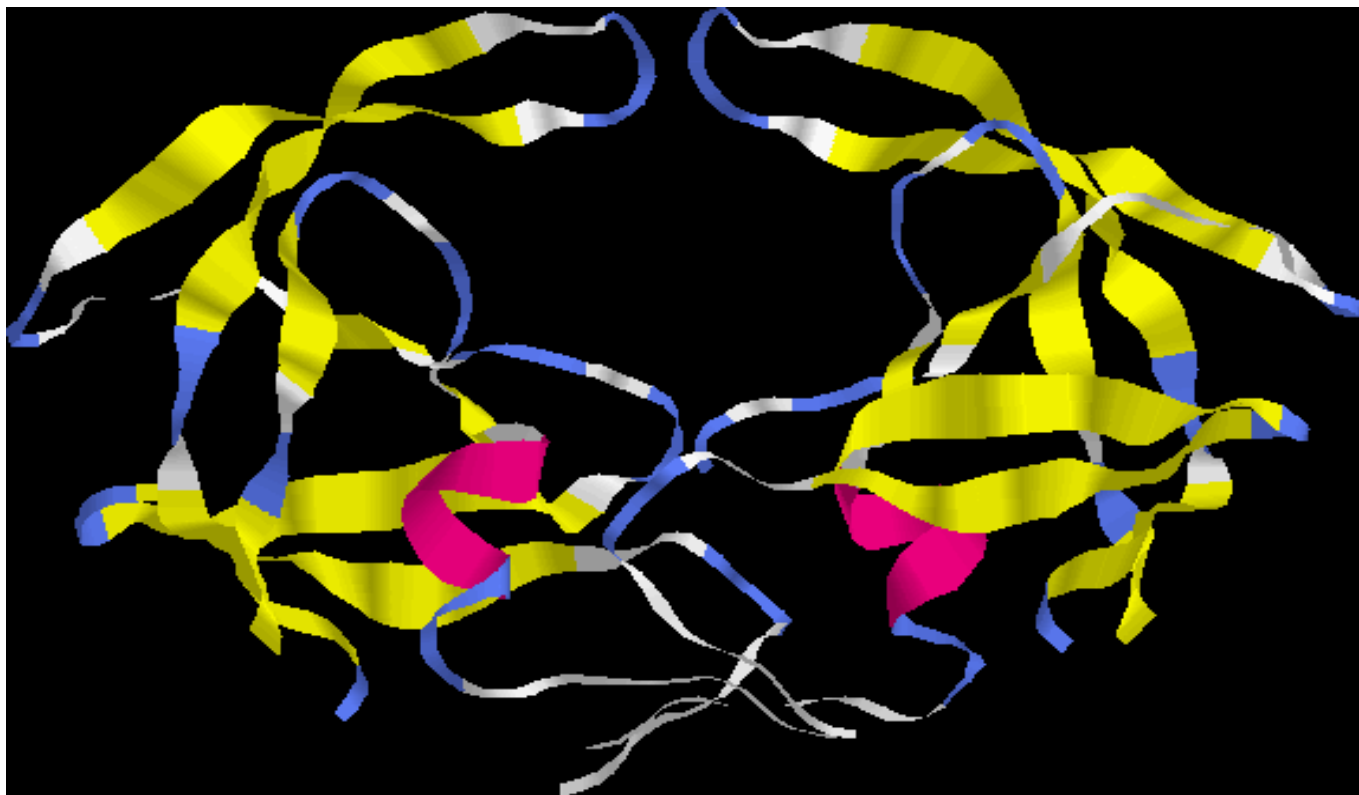


FIG. 1. Structure of HIV-1 PR [5].

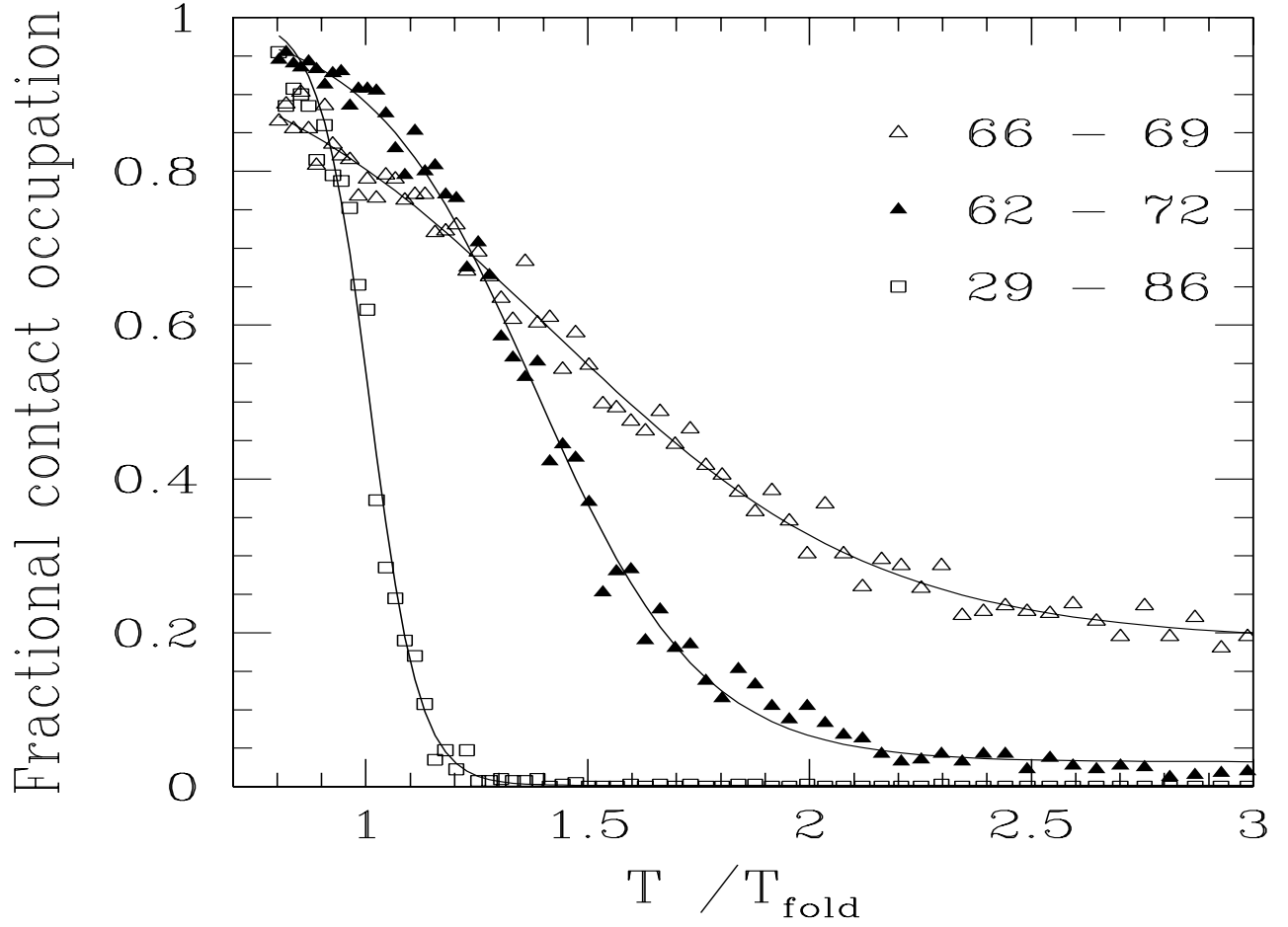


FIG. 2. Fractional occupation for three different native contacts. In all cases the fractional occupation approaches 1 as $T \rightarrow 0$ and vanishes for very large T . However, the rapidity of formation (slope at the inflexion point) is very different. The contact binding residues 66 and 69, located at the turn of β sheet 1, forms very gradually. The highest rapidity of formation of contacts in β_1 is observed for the pair 62, 72 (solid triangles). At the folding temperature, one of the highest formation rapidities is found in correspondence of the contact bonding residues 29 and 86 (open squares). The continuous curve is obtained from a smooth interpolation of the points.

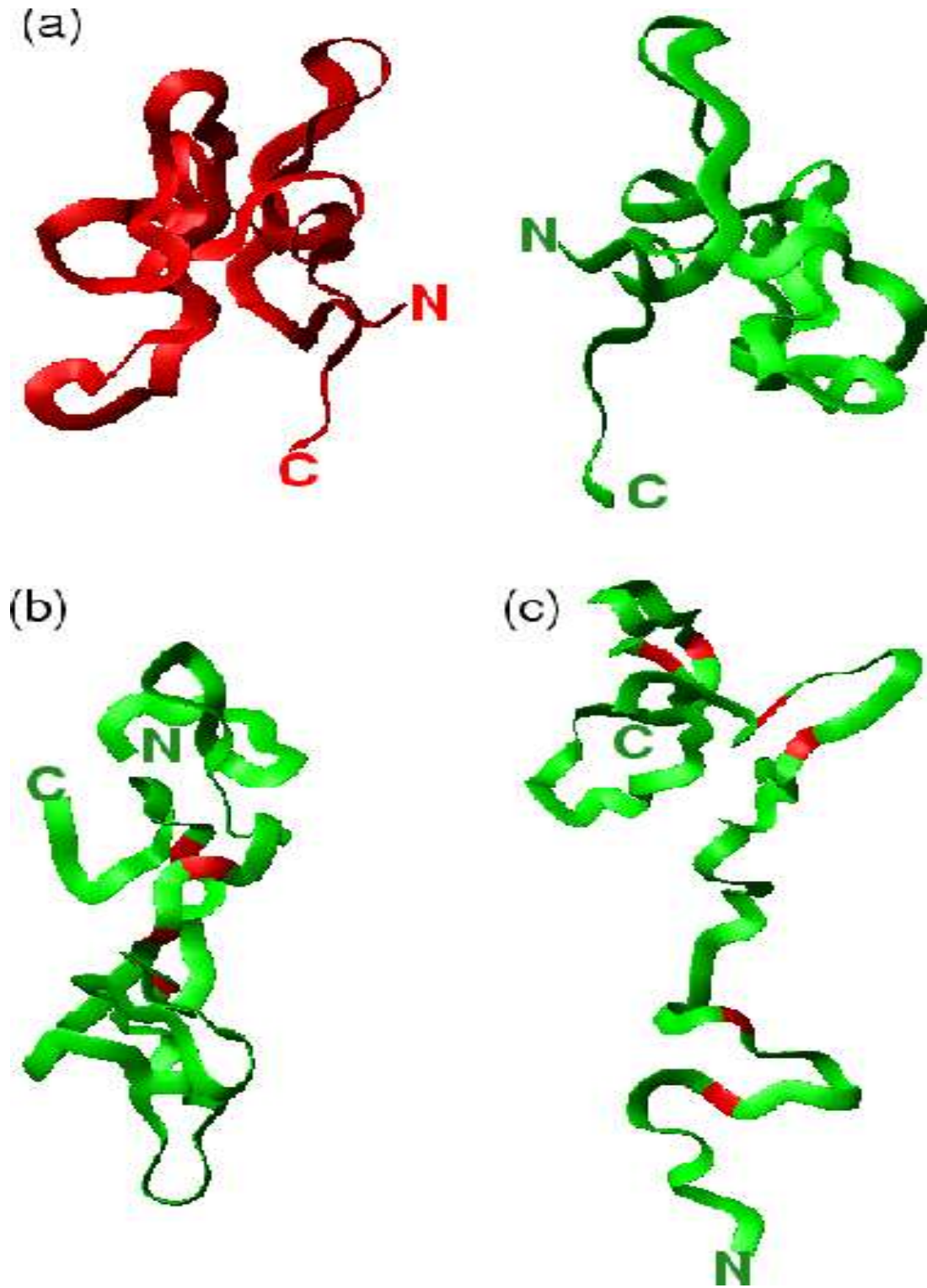


FIG. 3. Typical dimer conformations near the dissociation temperature T_{diss} (a). Typical monomer structures at the folding transition, T_{fold} (b) (key residues 29, 32, 76, 86 are highlighted in red) and at $1.3T_{fold}$ (c) (sites 11, 21, 46, 55, 61, 74 responsible for the initiation of the beta sheets are shown in red.)

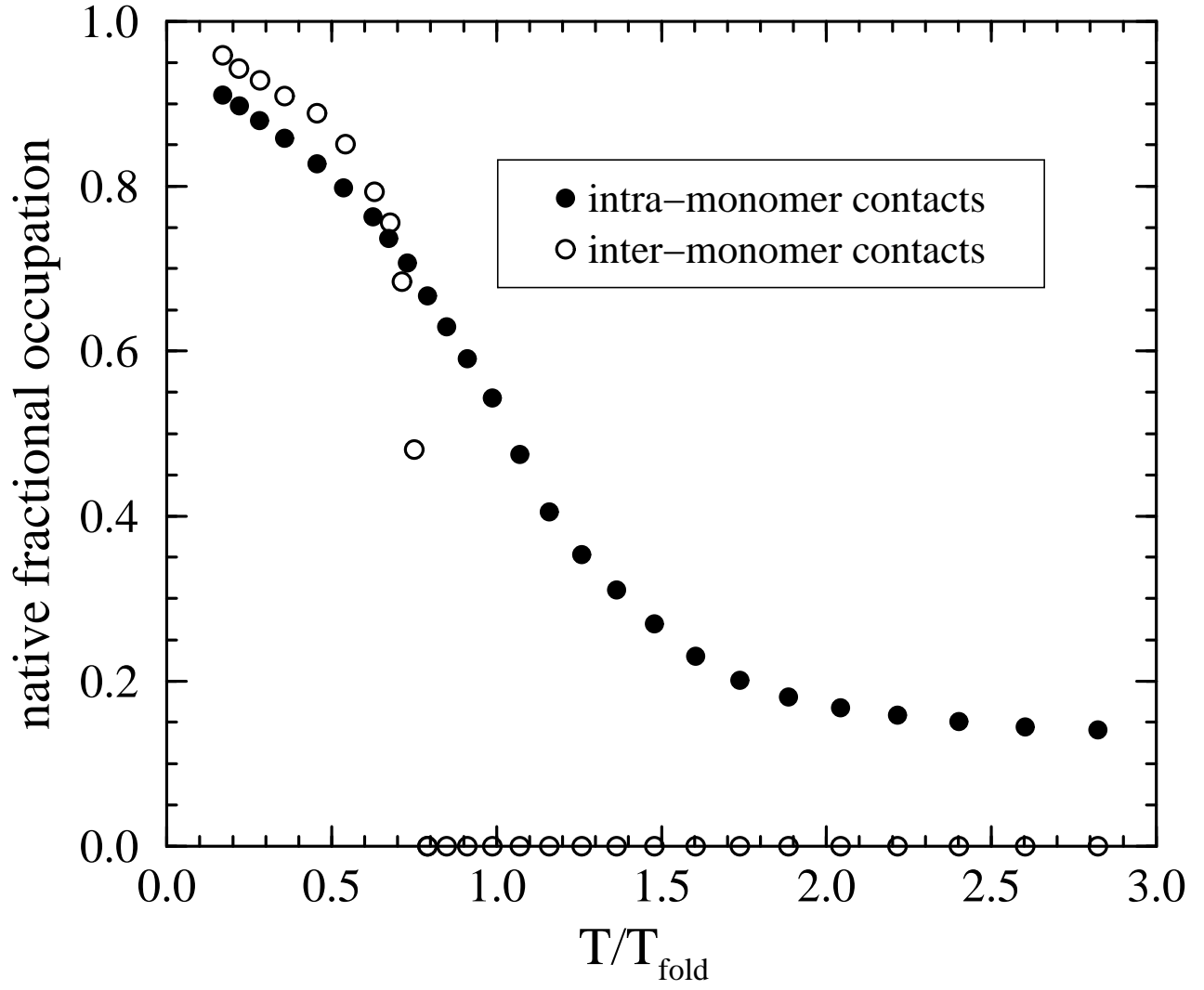


FIG. 4. Behaviour, as a function of temperature, of the average fractional occupation of native contacts within each HIV-1 PR monomer (solid circles) and at the interface between the two monomeric units (open circles). The dissociation of the two subunits is clearly seen to occur at $T/T_{fold} = 0.6$.

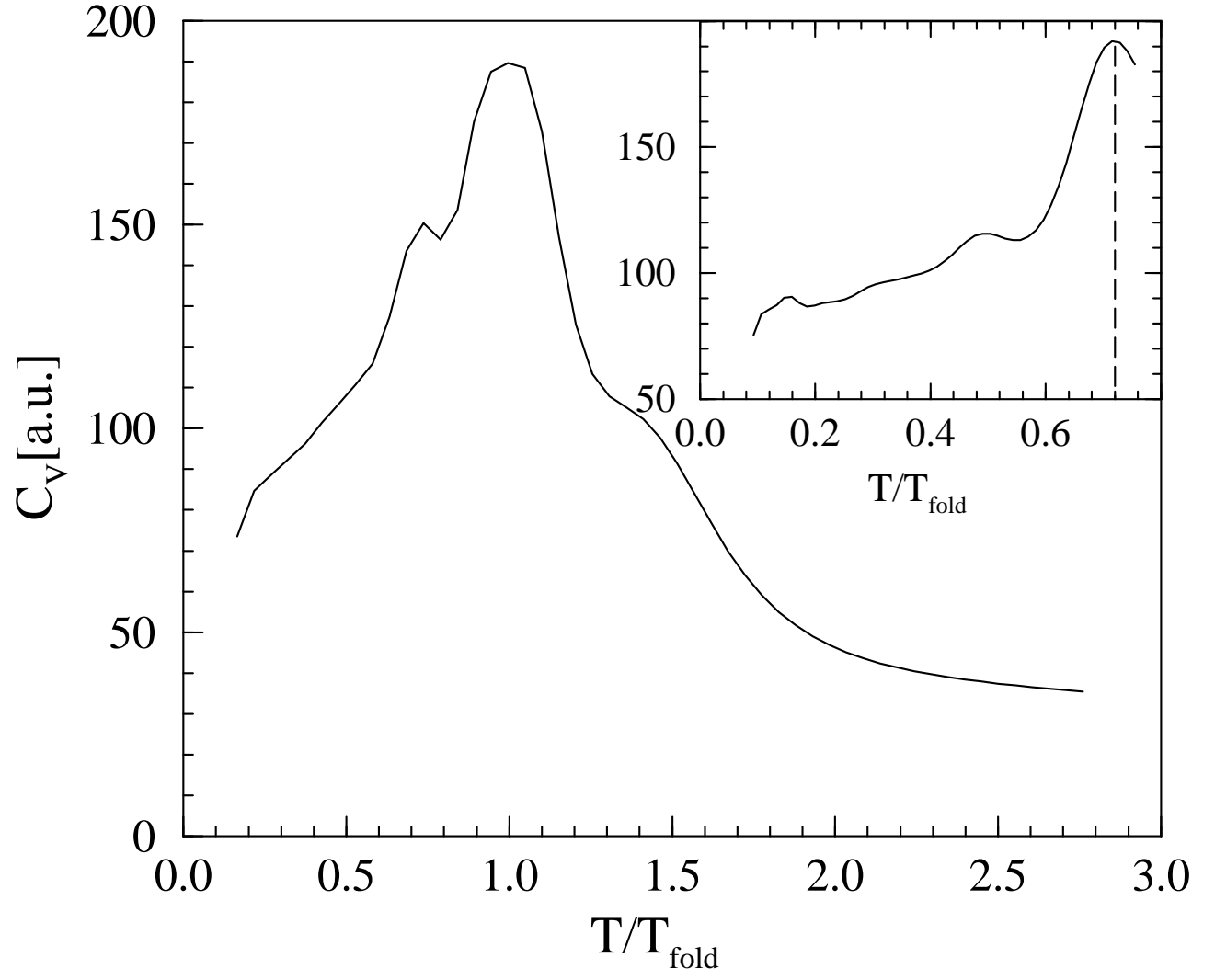


FIG. 5. Specific heat of the HIV-PR single monomer. The dimer specific heat at temperatures below the T_{diss} is shown in the inset.

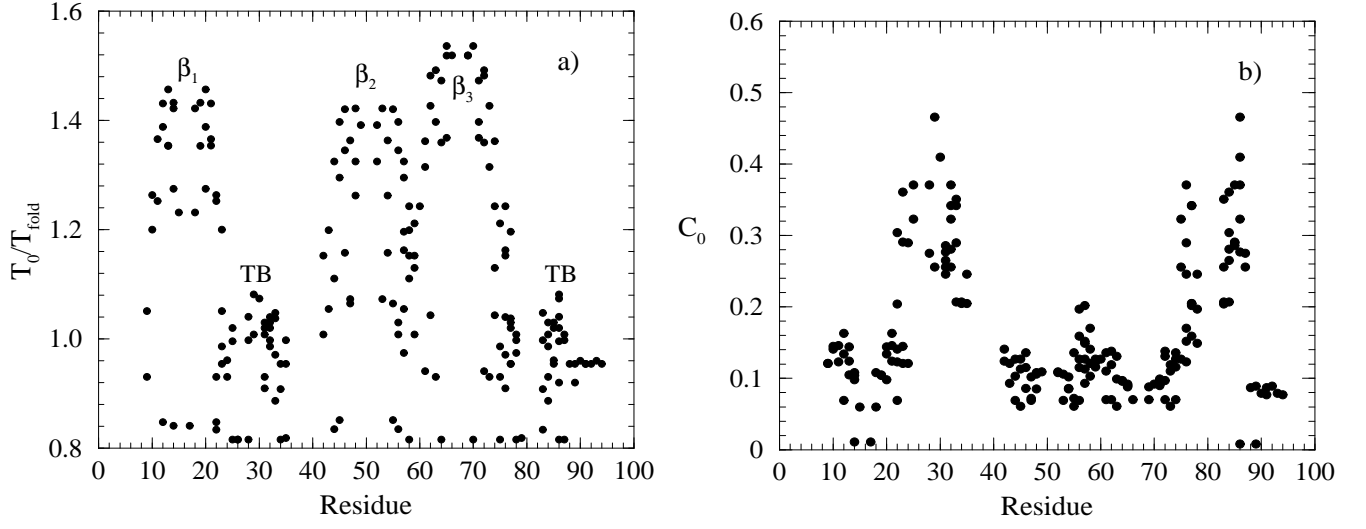


FIG. 6. (a) Characteristic temperatures T_0 (a) and maximum “rapidity” C_0 associated to each native contact versus the amino acid position sharing the contact. (b) Distribution of the values of the maximum rapidity C_0 of contacts involving each residue.

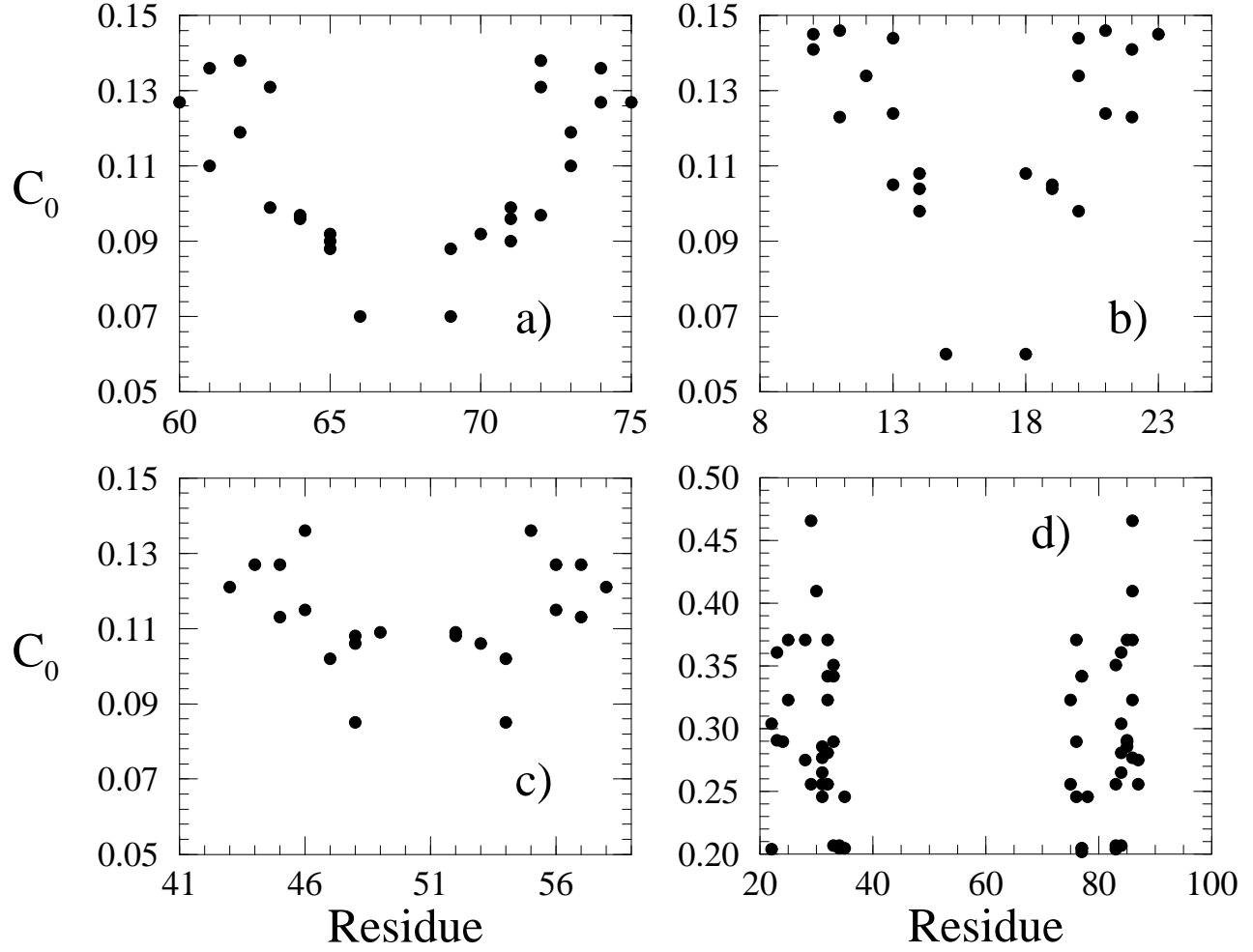


FIG. 7. Formation “rapidity” C_0 , for contacts in the four subregions of Fig. 6a. In order of decreasing formation temperature data are shown for a) β_3 , b) β_1 , c) β_2 and d) TB. Notice that the scale of C_0 depends on temperatures. The highest C_0 ’s for each of the regions increase as the temperature T_0 decreases.

Bottleneck	Key sites
TB	22, 29, 32, 76, 84, 86
β_1	10,11,13,20,21,23
β_2	44,45,46,55,56,57
β_3	61,62,63,72,74

TABLE I. Key sites for the four bottlenecks. For each bottleneck, only the sites in the top three pairs of contacts have been reported.

Name	Point Mutations	Bottlenecks
RTN [30,31]	20 , 33, 35, 36, 46 , 54, 63 , 71, 82, 84 , 90	TB, β_1 , β_2 , β_3
NLF [32]	30, 46 , 63 , 71, 77, 84 ,	TB, β_2 , β_3
IND [5,33]	10 , 32 , 46 , 63 , 71, 82, 84	TB, β_1 , β_2 , β_3
SQV [5,33,34]	10 , 46 , 48, 63 , 71, 82, 84 , 90	TB, β_1 , β_2 , β_3
APR [3]	46 , 63 , 82, 84	TB, β_2 , β_3

TABLE II. Mutations in the protease associated with FDA-approved drug resistance [4]. Sites highlighted in boldface are those involved in the folding bottlenecks as predicted in our approach. β_i refers to the bottleneck associated to the formation of the i -th β -sheet, whereas TB refers to the bottleneck occurring at folding transition temperature T_{fold}